

Concordance of Changes in Metabolic Pathways Based on Plasma Metabolomics and Skeletal Muscle Transcriptomics in Type 1 Diabetes

Tumpa Dutta,^{1,2} High Seng Chai,³ Lawrence E. Ward,² Aditya Ghosh,² Xuan-Mai T. Persson,² G. Charles Ford,² Yogish C. Kudva,¹ Zhifu Sun,³ Yan W. Asmann,³ Jean-Pierre A. Kocher,³ and K. Sreekumaran Nair^{1,2}

Insulin regulates many cellular processes, but the full impact of insulin deficiency on cellular functions remains to be defined. Applying a mass spectrometry-based nontargeted metabolomics approach, we report here alterations of 330 plasma metabolites representing 33 metabolic pathways during an 8-h insulin deprivation in type 1 diabetic individuals. These pathways included those known to be affected by insulin such as glucose, amino acid and lipid metabolism, Krebs cycle, and immune responses and those hitherto unknown to be altered including prostaglandin, arachidonic acid, leukotrienes, neurotransmitters, nucleotides, and anti-inflammatory responses. A significant concordance of metabolome and skeletal muscle transcriptome-based pathways supports an assumption that plasma metabolites are chemical fingerprints of cellular events. Although insulin treatment normalized plasma glucose and many other metabolites, there were 71 metabolites and 24 pathways that differed between nondiabetes and insulin-treated type 1 diabetes. Confirmation of many known pathways altered by insulin using a single blood test offers confidence in the current approach. Future research needs to be focused on newly discovered pathways affected by insulin deficiency and systemic insulin treatment to determine whether they contribute to the high morbidity and mortality in T1D despite insulin treatment. *Diabetes* 61:1004–1016, 2012

Insulin is critical for regulation of many cellular processes, although the most extensively studied effect of insulin is on glucose homeostasis. Absolute insulin deficiency in type 1 diabetes (T1D) causes profound alterations in carbohydrate, lipid, and protein metabolism (1,2). Insulin plays a key regulatory role in the transcription (3,4), translation (5), and posttranslational modification of proteins (6,7). Metabolites are the downstream end product of genome, transcriptome, and proteome variability of a biological system (8). Therefore, the metabolite fingerprint should give a direct specific measure of an altered physiological phenomenon (9–11).

Animal and human studies have shown the effects of the alterations in glucose tolerance and insulin sensitivity on plasma and urine metabolites (12–14). Nuclear magnetic

resonance-based nontargeted metabolomic profiling of human serum failed to distinguish between prediabetic individuals with impaired glucose tolerance and those with normal glucose tolerance (12,13). In contrast, an ultra-performance liquid chromatography quadrupole time-of-flight mass spectrometry (UPLC-ToF MS)-based comprehensive metabolomic profiling approach was found to discriminate between impaired and normal glucose tolerance (15). These emerging technologies have enabled researchers to identify biomarkers (14) to predict the risk for onset of diabetes that will help to develop strategies to prevent this disease and its complications.

With use of a model of insulin deficiency in T1D, alterations in specific metabolic pathways due to insulin deficiency have been reported (12,16–19). Although systemic insulin treatment normalizes glucose, it remains unclear whether other metabolic abnormalities are also corrected. It is well-known that systemic insulin treatment not only causes relative hyperinsulinemia but also alters the normal hepatic:peripheral insulin ratio of 2:1 that is normally present in nondiabetic (ND) individuals (19). We therefore sought to determine whether systemic insulin treatment normalizes all metabolic alterations in T1D.

In the current study, a nontargeted UPLC-ToF MS-based metabolomics approach was applied to determine the effects of insulin deficiency on metabolites and pathways in T1D individuals. We compared plasma metabolites in T1D during systemic insulin treatment (I^+) and following 8 h of insulin withdrawal (I^-) in comparison with matched ND individuals. Since skeletal muscle is a key target organ of insulin action (4,20,21), we sought to determine whether pathways based on the skeletal muscle transcriptome have any concordance with those of plasma metabolites in T1D during insulin deficiency.

RESEARCH DESIGN AND METHODS

Seven C-peptide-negative T1D subjects were studied on two occasions: one during insulin treatment and the other following withdrawal of insulin for 8 h and compared with matched healthy ND participants (Table 1). All study volunteers were screened with a detailed medical history, physical exam, and hematological and biochemical profile (22–24). The list of medications taken by the participants is given in Supplementary Table 1. On the insulin treatment study day, insulin was infused into a forearm vein to maintain blood glucose between 4.44 and 5.56 mmol/L overnight until 1200 h the next day. On the insulin deprivation study day, insulin was discontinued for 8.6 ± 0.6 h starting at 0400 h. ND participants were kept on a saline infusion from the evening following their meal. Arterialized venous blood was obtained from a catheterized hand vein maintained at 60°C using a hot box for the duration of the study. Plasma samples were stored at -80°C until analysis. Percutaneous needle biopsies were performed under local anesthesia as previously described (25) with the muscle specimens immediately frozen in liquid nitrogen and stored at -80°C until analysis.

From the ¹Division of Endocrinology and Endocrine Research Unit Rochester, Rochester, Minnesota; the ²Center for Translational Science Activities Metabolomics Core Facility, Mayo Clinic, Rochester, Minnesota; and ³Biomedical Statistics and Informatics, Mayo Clinic, Rochester, Minnesota.

Corresponding author: K. Sreekumaran Nair, nair.sree@mayo.edu.

Received 11 July 2011 and accepted 22 November 2011.

DOI: 10.2337/db11-0874

This article contains Supplementary Data online at <http://diabetes.diabetesjournals.org/lookup/suppl/doi:10.2337/db11-0874/-/DC1>.

© 2012 by the American Diabetes Association. Readers may use this article as long as the work is properly cited, the use is educational and not for profit, and the work is not altered. See <http://creativecommons.org/licenses/by-nc-nd/3.0/> for details.

TABLE 1
Characteristics of study participants

Variables	ND	T1D (I ⁻)	T1D	T1D (I ⁺)
<i>n</i>	7		7	
Age (years)	29.7 ± 3		30 ± 3	
Weight (kg)	81 ± 6.4		78.2 ± 5	
BMI (kg/m ²)	25 ± 1.1		26.2 ± 1.3	
Fat mass (%)	33.2 ± 4		31.6 ± 4.1	
HbA _{1c} (%)	5.0 ± 0.05		7.2 ± 0.5*	
Type 1 diabetes duration (years)			18.7 ± 4	
Glucose (mmol/L)	4.9 ± 0.1	17.0 ± 0.6 ^{a,b}		5.2 ± 0.2
Glucagon (ng/L)	99.0 ± 19.0	82.6 ± 17.3		50.3 ± 6.8 ^a
Insulin (pmol/L)	23.4 ± 4.52	3.9 ± 1.36 ^{a,b}		69.8 ± 17.8 ^a

*Data are means ± SE for seven participants (three women and four men)/group. ^a*P* ≤ 0.05 vs. ND. ^b*P* ≤ 0.05 vs. T1D (I⁺).

Metabolomic profiling

Sample preparation. Plasma quality-control samples used in the study were prepared from pooled plasma spiked with a selection of metabolites to mimic elevated levels of metabolites during I⁻ condition. Plasma was spiked with a standard mixture (3:1 ratio of plasma to spiking solution) containing 100 µg/mL niacin, hypoxanthine, leucine, isoleucine, phenylalanine, tryptophan, citric acid, glucose, hippuric acid, and taurocholic acid dissolved in 1:1 acetonitrile/water. All plasma samples (200 µL) were thawed on ice at 4°C followed by deproteinization with methanol (1:4 ratio of plasma to methanol) and vortexed for 10 s, followed by incubation at -20°C for 2 h. The samples were then centrifuged at 15,871*g* for 30 min at 4°C. The supernatants were lyophilized (Savant, Holbrook, NY) and stored at -20°C prior to analysis. The samples were reconstituted in 50% H₂O/acetonitrile and passed through a Microcon YM3 filter (Millipore Corporation). The supernatants were transferred to analytical vials, stored in the autosampler at 4°C, and analyzed within 48 h of reconstitution in buffer.

The liquid chromatography platform consisted of an Acquity UPLC system (Waters, Milford, MA). Plasma metabolite separation was achieved using both hydrophilic interaction chromatography (ethylene-bridged hybrid 2.1 × 150 mm, 1.7 µm; Waters) and reversed-phase liquid chromatography C18 (high-strength silica 2.1 × 150 mm, 1.8 µm; Waters). For each column, the run time was 20 min at a flow rate of 400 µL/min. Reverse-phase chromatography was performed using 99% solvent A (5 mmol/L NH₄ acetate, 0.1% formic acid, and 1% acetonitrile) to 100% solvent B (95% acetonitrile with 0.1% formic acid). The gradient was 0 min, 0% B; 1 min, 0% B; 3 min, 5% B; 13.0 min, 100% B; 16 min, 100% B; 16.5 min, 0% B; and 20 min, 0% B. The hydrophilic interaction chromatography gradient was as follows: 0 min, 100% B; 1 min, 100% B; 5 min, 90% B; 13.0 min, 0% B; 16 min, 0% B; 16.5 min, 100% B; and 20 min, 100% B. Other LC parameters were injection volume 5 µL and column temperature 50°C. Each sample was injected in triplicate with blank injections between each sample. Quality controls and standards were run at the beginning and end of the sequence.

Mass spectrometry. A 6220 ToF MS (Agilent Technologies) was operated in both positive and negative electrospray ionization modes using a scan range of 50–1,200 *m/z*. The mass accuracy and mass resolution were <5 parts per million (ppm) and ~20,000, respectively. The instrument settings were as follows: nebulizer gas temperature 325°C, capillary voltage 3.5 kV, capillary temperature 300°C, fragmentor voltage 150 V, skimmer voltage 58 V, octapole voltage 250 V, cycle time 0.5 s, and run time 15.0 min.

Data preprocessing. All raw data files were converted to compound exchange file format using Masshunter DA reprocessor software (Agilent Technologies). Mass Profiler Professional (Agilent) was used for data alignment and to convert each metabolite feature (*m/z* × intensity × time) into a matrix of detected peaks versus compound identification. Each sample was normalized to the median of the baseline and log 2 transformed. Default settings were used with the exception of signal-to-noise ratio threshold (3), mass limit (0.0025 units), and time limit (9 s).

The resulting metabolites were identified against the METLIN metabolite database using a detection window of ≤5 ppm. Putative identification of each metabolite was made based on mass accuracy (*m/z*) Chemical Abstracts Service (CAS), Kyoto Encyclopedia of Genes and Genomes (KEGG), Human Metabolome Project (HMP) database, and LIPID MAPS identifiers (26,27).

Method performance was evaluated for the ten metabolite standards with respect to limit of detection, linearity, reproducibility, and mass accuracy. Linearity was evaluated using the linear regression of the observed signal with respect to concentration, with a lower limit of 10 ng/mL set as the limit of detection. In addition, the 10 ng/mL mix was run three times each day over 5 days during a period of 1 month to determine inter- and intra-assay variation.

Analysis of gene transcripts using GeneChips. RNA was extracted from frozen muscle samples (50 mg) using the RNeasy Fibrous Tissue kit (Qiagen) following the manufacturer's instructions. Gene transcript profiles were measured using high-density oligonucleotide microarrays containing probes for 54,675 transcripts and expressed sequence tags (HG133 plus 2.0 GeneChip arrays; Affymetrix, Santa Clara, CA). GeneChip data were subjected to invariant probe set normalization (24). Differences between the I⁻ T1D and I⁺ T1D/ND groups were evaluated by paired *t* test (24,28). We opted to focus on significantly altered pathways and functional gene sets rather than individual genes.

To validate the findings of the gene array results and to quantify other genes of interest, transcript levels of selected genes were analyzed by real-time quantitative PCR (Applied Biosystems 7900) as previously described (24,29). The primers and probes used were cytochrome *c* oxidase (COX) subunits COX5B and COX10, ubiquinol cytochrome *c* reductase 6.4-kDa subunit, and uncoupling proteins (UCP 2/3) and ATP5F1 subunit (25). The abundance of the target gene was normalized to 28S (29).

Statistical analysis. One of the challenges in the analysis of metabolomics data resides in the substantial missing values in the dataset. The compounds detected in at least ≥50% of the samples in any treatment group were selected for differential expression analyses. Then, two approaches based on two different assumptions were used to handle missing values. First, missing values were assumed to be of very low abundance (at the limit of experimental detection) or zero abundance and were replaced by 1.0 before applying log 2 transformation. The second approach involved the use of parametric imputation models to provide estimates of the missing values. Imputation leverages the pattern of expression between a set of correlated metabolite features to predict the missing values of metabolites. In order to reduce the uncertainty associated with estimating missing values, only metabolites present in at least 50% of all the samples and at least five samples in each study group were used for imputation. Each metabolite feature was independently imputed from the 10 most closely correlated metabolites from the same experimental mode. Missing value estimation was carried out using Markov Chain Monte Carlo methods included in R software with 100 imputations and 50 iterations. Imputation models were set to account for treatment groups and replicate samples.

The complete datasets resulting from both approaches were analyzed using random intercept models to account for the multiple measurements that were taken from each sample. Separate models were fitted for each pairwise treatment group comparison. Results from multiple imputations were combined with methods proposed by Rubin (30). All statistical calculations were performed using the statistics software package R. In particular, the *mi* and *lme4* packages were used for multiple imputation and random-effect model fitting, respectively. Identified compounds that were differentially expressed across treatment groups were used for pathway analysis.

Hierarchical cluster analysis of metabolites was performed to reveal associations between replicate biological samples within a group based on the similarity of their mass abundance profiles. Hierarchical cluster analysis was performed on the log 2-transformed, one-way ANOVA data set. A heat map was generated, wherein each column depicts a sample and each row represents a metabolite, with the relative change color coded (Fig. 1).

Pathway analysis. The differentially expressed metabolites were analyzed for pathway enrichment using MetaCore (Genego, St. Joseph, MI) (31). Metabolite identifiers (CAS and KEGG) were used for each metabolite including name and molecular weight in addition to fold change and differential *P* value. The *P* value from the hypergeometric test, generated by Metacore, represents the

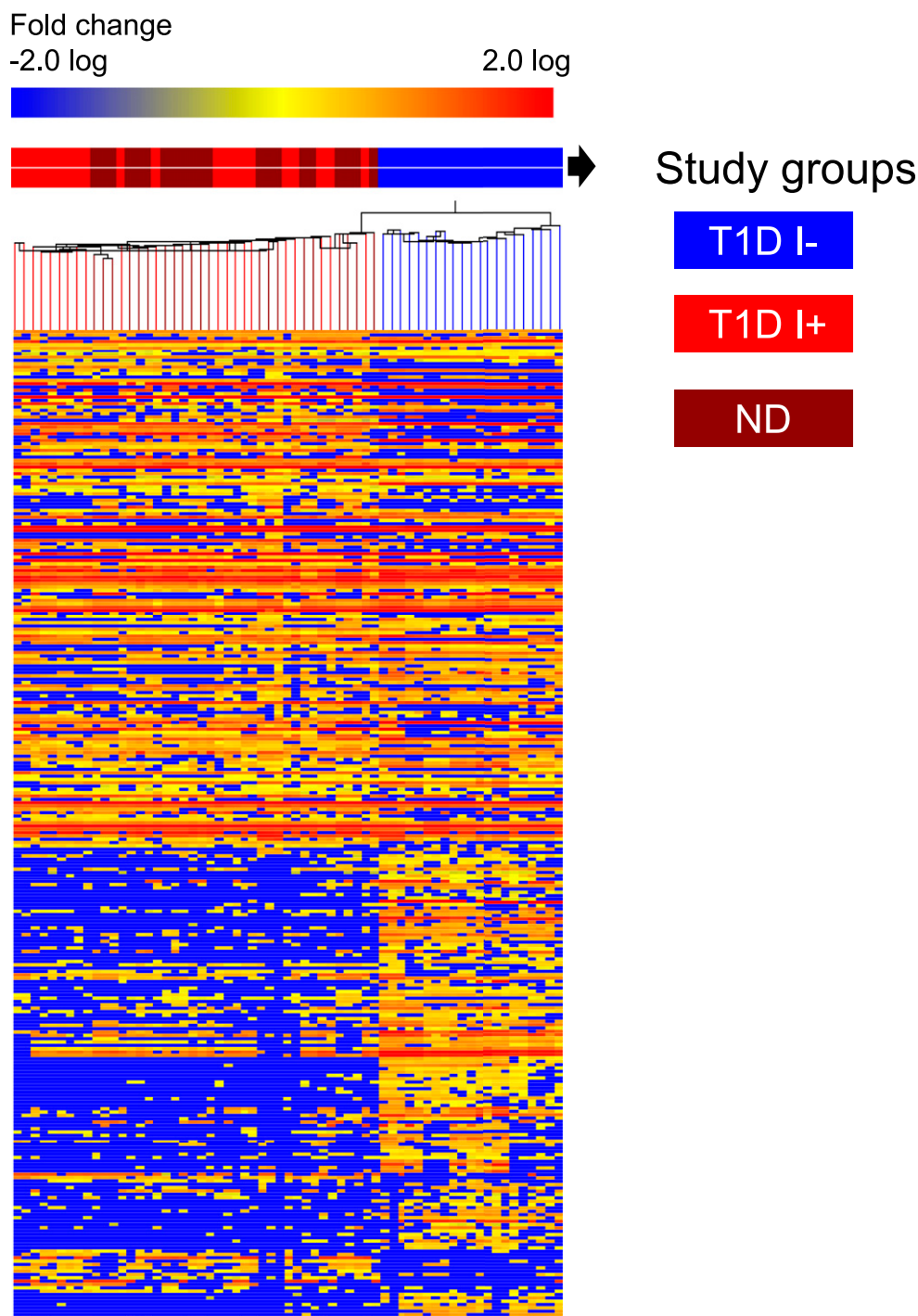


FIG. 1. Heat map analysis of plasma metabolites in T1D during insulin deficiency (I^-) and insulin treatment (I^+) and comparison with ND. Metabolite perturbations in plasma were calculated based on the median for each metabolite level of three independent biological replicates of plasma samples from each study participant. Each row represents a metabolite, and each column depicts a subject. The study groups are color coded as follows: insulin-deprived (I^-) T1D is denoted in blue, insulin-treated (I^+) T1D is denoted in red, and ND groups are denoted in maroon. The fold change in metabolite levels is color coded: red pixels, upregulation; blue, downregulation; yellow, no significant change. Metabolites such as acetate, lactate, acetoacetate, hydroxybutyrate, gluconate, hydroxy adipate, carnitines, glucosamine, and taurocholate including amino acid (e.g., leucine, isoleucine, valine, *N*-methyl histidine, keto glutarate, glutamate, alanine, phenylalanine) were all found to be elevated in I^- T1D (Supplementary Table 4). A consistent decrease was observed in other metabolites, e.g., hydroxypyridine, nicotinamide, hydroxyl nicotinic acid, adipate, methylthioribose, uridine, xanthine, hypoxanthine, methylguanosine, *N*-acetyl tryptophan, pipercolate, homoserine, aldosterone, arachidonyl lysolecithin, phosphoethanolamine, etc.

enrichment of certain metabolites in a pathway. A P value ≤ 0.05 is indicative of significant enrichment. The ratio of significantly changed metabolites in the pathway to total number of metabolites in a pathway was also calculated. A false discovery rate of < 0.15 was also applied. A comparison of canonical pathways was also made between the metabolome and transcriptome studies.

RESULTS

Clinical and biochemical characteristics of participants are given in Table 1. Significantly higher levels of HbA_{1c} were noted in T1D. Plasma glucose levels remained significantly higher in I^- , but insulin concentration was

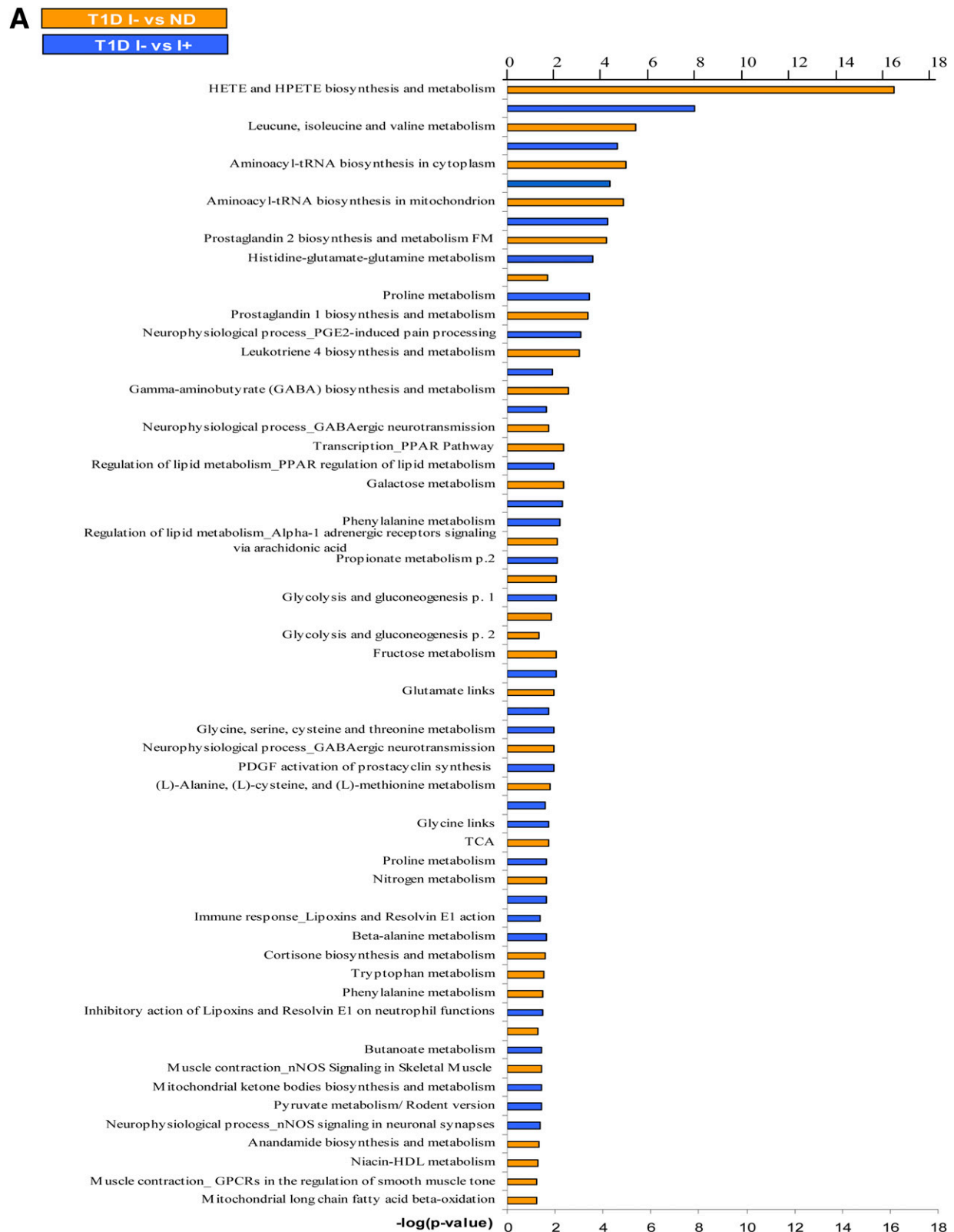


FIG. 2. A: The effect of differential regulation of metabolites on the canonical pathways during I^- in T1D in comparison with I^+ T1D and ND. The significance of the pathways was evaluated using P values and false discovery rate <0.05 . **B:** Altered canonical pathways following insulin treatment in T1D in comparison with ND. *Metabolic pathways that were observed exclusively after systemic insulin treatment. The significance of the pathways was evaluated using P values and false discovery rate <0.05 . nNOS, neuronal nitric oxide synthase; PDGF, platelet-derived growth factor; TCA, tricarboxylic acid; GPCR, G protein-coupled receptor; FM, function and metabolism.

B

#	Maps	0	2	4	6	-log(pValue)	pValue
1	HETE and HPETE biosynthesis and metabolism	████████████████████					1.524e-6
2	Prostaglandin 2 biosynthesis and metabolism FM	████████████████████					1.074e-5
3	Histidine-glutamate-glutamine metabolism	████████████████████					5.506e-5
4	Neurophysiological process GABAergic neurotransmission	████████████████████					6.324e-4
5	Leucine, isoleucine and valine metabolism	████████████████████					9.029e-4
6	Gamma-aminobutyrate (GABA) biosynthesis and metabolism	████████████████████					9.822e-4
7	Propionate metabolism p.2	████████████████████					3.273e-3
8	Immune response PGE2 in immune and neuroendocrine system interactions*	████████████████████					2.956e-3
9	Leukotriene 4 biosynthesis and metabolism	████████████████████					3.217e-3
10	Niacin-HDL metabolism	████████████████████					4.093e-3
11	TCA	████████████████████					5.494e-3
12	Cortisone biosynthesis and metabolism	████████████████████					1.152e-2
13	Regulation of lipid metabolism Alpha-1 adrenergic receptors signaling via arachidonic acid	████████████████████					1.647e-2
14	Androstenedione and testosterone biosynthesis and metabolism p.3*	████████████████████					1.938e-2
15	Androstenedione and testosterone biosynthesis and metabolism p.3/ Rodent version*	████████████████████					2.336e-2
16	NAD metabolism*	████████████████████					2.552e-2
17	Muscle contraction GPCRs in the regulation of smooth muscle tone*	████████████████████					2.877e-2
18	Chemotaxis Inhibitory action of lipoxins on IL-8- and Leukotriene B4-induced neutrophil migration*	████████████████████					3.425e-2
19	Immune response Inhibitory action of lipoxins on superoxide production induced by IL-8 and Leukotriene B4 in neutrophils*	████████████████████					3.091e-2
20	(L)-Alanine, (L)-cysteine, and (L)-methionine metabolism	████████████████████					4.338e-2
21	Muscle contraction nNOS Signaling in Skeletal Muscle	████████████████████					5.435e-2
22	Aminoacyl-tRNA biosynthesis in cytoplasm	████████████████████					4.684e-2
23	Aminoacyl-tRNA biosynthesis in mitochondrion	████████████████████					5.138e-2
24	Transcription PPAR Pathway	████████████████████					5.360e-2

FIG. 2. Continued

significantly lower. Insulin concentration was higher in I^+ than in ND. Glucagon concentration was significantly lower in I^+ than in ND with similar glucose levels. Bicarbonate levels were not significantly different between the two groups, indicating that I^- T1D subjects were not in metabolic acidosis, although β -hydroxy butyrate concentration was higher in I^- than in I^+ , showing that fatty acid metabolism was elevated. No difference was detected in the other physiological parameters reflecting kidney function, total protein, and albumin (data not shown) in plasma.

Plasma metabolome. The coefficient of variation of retention times of the standard compounds was $<5\%$, and the mass accuracy was ≤ 5 ppm (Supplementary Tables 2 and 3). Metabolic profiling identified a total of 402 compounds including metabolites, peptide fragments, and drug molecules (data not shown). Of these, 330 metabolites were detected and identified in all three study groups: I^- , I^+ , and ND (Supplementary Table 4). Sixty-nine metabolites that were confirmed based on comparison with standards and retention time are listed in Supplementary Table 3. The identification of the other 261 metabolites (Supplementary Table 4) was based on accurate mass measurements using database searches.

A heat map was generated using identified and unidentified metabolites (Fig. 1). The heat map revealed considerable differences between I^- , I^+ , and ND, showing alterations in the natural abundance of several metabolites in plasma. The heat map demonstrated that replicate samples belonging to the different study groups were clustered.

Impact of insulin deprivation. The comprehensive profiling approach of paired analysis (I^- vs. I^+ and I^- vs. ND)

showed alterations of 302 known plasma metabolites in T1D (I^-) individuals, of which 176 were significant ($P < 0.05$) (Supplementary Table 5). The metabolite classes that were found to be significantly altered between I^- and I^+ include plasma amino acids, branch-chain amino acids (BCAAs), lipid metabolites, bile acids, purines, pyrimidines, Krebs (tricarboxylic acid) cycle and carbohydrate metabolites, transcription of peroxisome proliferator-activated receptor (PPAR), and vitamins including steroids and ecosanoids. Consistent changes were also observed when the metabolite plasma levels in I^- were compared with ND (Supplementary Table 6).

Pathway-enrichment analysis. Analysis of identified metabolites showed that >33 canonical pathways ($P \leq 0.05$) were perturbed during insulin deficiency (Fig. 2A). Table 2 shows a short list of selected metabolic pathways that were affected by differential regulation of metabolites during insulin deficiency in comparison with I^+ and ND. A comparison of pathway-enrichment analysis before and after multiple imputation analysis of paired study groups was also performed and showed that the overall pathway findings remained the same but the statistical inference was changed. The P values of the pathways involving andamide, prostaglandin, γ -amino butyrate (GABA), cortisone biosynthesis, and metabolism were decreased, whereas hydroxyeicosatetraenoic acid (HETE) and hydroperoxyeicosatetraenoic acid (HPETE) biosynthesis, leukotriene metabolism including tryptophan, and butanoate metabolism were increased significantly after imputation (data not shown).

Effect of systemic insulin treatment. In order to identify whether insulin treatment ameliorates the metabolic pattern in T1D, the metabolic fingerprint of I^+ was compared with that of ND. Paired analysis of I^+ versus

TABLE 2
Implicated canonical pathways affected by differential regulation of metabolites during I⁻ in T1D in comparison with I⁺ T1D and ND

Maps	Regulation	<i>P</i>	Ratio
Leucine, isoleucine, and valine metabolism (BCAA)	Up	3.036e ⁻⁹	10:54
Prostaglandin, HETE, and HPETE biosynthesis and metabolism	Up	6.892e ⁻⁸	12:80
Histidine-glutamate-glutamine metabolism	Up	5.862e ⁻⁵	8:96
Aminoacyl-tRNA biosynthesis in cytoplasm/mitochondria	Up	6.315e ⁻⁵	8:97
Propionate metabolism	Up	6.459e ⁻⁵	7:72
Neurophysiological process: GABAergic neurotransmission	Up	6.680e ⁻⁵	6:50
GABA biosynthesis and metabolism	Up	1.151e ⁻⁴	6:55
Proline metabolism	Up	1.022e ⁻³	5:55
(L)-Alanine, (L)-cysteine, and (L)-methionine metabolism	Up	1.109e ⁻³	5:56
β-Alanine metabolism	Up	1.412e ⁻³	4:35
Galactose metabolism	Up	1.758e ⁻³	5:62
Fructose metabolism	Up	3.608e ⁻³	5:73
Anandamide biosynthesis and metabolism	Up	3.906e ⁻³	4:46
Glycolysis and gluconeogenesis	Up	3.906e ⁻³	4:46
Tyrosine metabolism	Up	8.347e ⁻³	5:89
Cortisone biosynthesis and metabolism	Up	1.187e ⁻²	4:63
<i>N</i> -Acylethanolamines: <i>N</i> -Acyltransferase pathway	Up	1.195e ⁻²	3:34
Phenylalanine metabolism	Up	1.539e ⁻²	4:68
Regulation of lipid metabolism: PPAR regulation of lipid metabolism	Up	2.114e ⁻²	3:42
Methionine-cysteine-glutamate metabolism	Up	2.250e ⁻²	3:43
Regulation of lipid metabolism: insulin regulation of fatty acid metabolism	Up	3.561e ⁻²	4:88
Taurine and hypotaurine metabolism	Up	3.802e ⁻²	3:22
Mitochondrial ketone bodies biosynthesis and metabolism	Up	5.521e ⁻²	3:27
Muscle contraction: eNOS signaling in skeletal muscle	Up	5.521e ⁻²	3:27
Butanoate metabolism	Up	6.385e ⁻²	3:65
Pyruvate metabolism	Up	6.623e ⁻²	3:66
Acetylcholine biosynthesis and metabolism	Up	7.457e ⁻²	2:32
Regulation of lipid metabolism: α-1 via arachidonic acid adrenergic receptors signaling	Up	7.614e ⁻²	3:70
Urea cycle	Up	7.614e ⁻²	3:70
Fatty acid ω oxidation	Up	8.284e ⁻²	2:34
Aspartate and asparagine metabolism	Up	8.398e ⁻²	3:73
Nitrogen metabolism	Up	8.708e ⁻²	5:35
Aminoacyl-tRNA biosynthesis in cytoplasm/mitochondria	Down	5.104e ⁻⁴	6:97
Catecholamine metabolism	Down	2.100e ⁻¹	2:74
CTP/UTP metabolism	Down	4.537e ⁻²	3:108
Regulation of lipid metabolism: α-1 via arachidonic acid adrenergic receptor signaling	Down	7.636e ⁻³	6:34

TABLE 2
Continued

Maps	Regulation	<i>P</i>	Ratio
Glycine, serine, cysteine, and threonine metabolism	Down	6.482e ⁻³	3:122
GTP-XTP metabolism	Down	2.758e ⁻³	3:90
Histidine-glutamate-glutamine metabolism	Down	3.664e ⁻²	3:96
Neurophysiological process: role of CDK5 in presynaptic signaling	Down	8.510e ⁻²	3:28
Niacin-HDL metabolism	Down	1.388e ⁻²	3:47
Pentose phosphate pathway	Down	1.525e ⁻²	3:52
Bile acid biosynthesis	Down	5.23e ⁻²	4:94
Phenylalanine metabolism	Down	2.268e ⁻³	3:68
Tryptophan metabolism	Down	4.238e ⁻²	4:104
Tyrosine metabolism	Down	2.552e ⁻²	3:64
Glutathione metabolism	Down	4.25e ⁻²	3:72
Ubiquinone metabolism	Down	2.264e ⁻²	3:74

The regulation was calculated on log 2-scaled values of I⁻ with respect to I⁺ and ND individuals. *P* value is the significance of the pathway, and ratio is the number of compounds identified to the total number of metabolites present in a pathway. eNOS, endothelial nitric oxide synthase; CTP, cytidine triphosphate; UTP, uridine 5'-triphosphate; GTP, guanosine 5'-triphosphate.

ND identified 241 altered metabolites, of which 71 were significant (*P* < 0.05) (Supplementary Table 7). This perturbation of pathways included eicosanoid metabolism, BCAA, immune response, prostaglandin-2 response, and the corresponding signaling pathways (Fig. 2B). The abnormalities in these pathways indicated that insulin treatment in T1D did not restore the metabolic alterations completely. In addition, systemic insulin treatment in T1D compared with ND showed a differential effect on seven metabolic pathways, which was not observed in comparison with the I⁻ state (Fig. 2B).

Correlation of metabolomics and transcriptomics in altered insulin action. Consistent differences between I⁻ and I⁺ T1D individuals based on quantitative PCR-based mRNA levels of COX5B, COX10, ubiquinol cytochrome *c* reductase, and ATP5F1 and mRNAs based on gene array have previously been reported (27). A total of 40,438 transcripts from gene array were included in the analysis, of which 2,355 and 1,775 transcripts were differentially expressed between I⁻ versus ND and I⁺ versus ND subjects, respectively (*P* < 0.05) (24). These genes were used as focus genes for pathway analysis.

Both transcriptome and metabolome levels were found to be affected by insulin deprivation in T1D. Therefore, the muscle gene transcriptome was compared with the plasma metabolome of the same participants under identical study conditions. Analysis of I⁻ versus ND for microarray and metabolomics profile identified several canonical pathways indicating similar directional changes, as shown in Fig. 3A. These implicated pathways, namely, transcription of PPAR, immune response related to prostaglandin-2, muscle contraction, lipid and carbohydrate metabolism, and inhibitory actions of lipoxins, showed a direct correlation of metabolites with transcriptome and their differential regulation during low insulin action. These pathways are clustered based on the gene-metabolite pathway associations.

In general, many pathways agreed between the ones based on metabolomics and transcriptome (Fig. 3A and B).

A



FIG. 3. Comparison of plasma metabolome with transcriptome of I⁻ versus ND (A) and I⁺ versus ND (B). The coclustering between the metabolomic changes and the transcripts of the corresponding muscle genes showed similar directional changes on the canonical pathways, although the statistical significance was different. The microarray/transcriptome data and the metabolome data are marked with an orange bar and blue bar, respectively. *Pathways used to build metabolic networks, as shown in Fig 4. EGF, epidermal growth factor; ERK, extracellular signal-related kinase; nNOS, neuronal nitric oxide synthase; PDGF, platelet-derived growth factor; TGF, transforming growth factor; GPCR, G protein-coupled receptor; LTD4, leukotriene receptor D4; HGF, hepatocyte growth factor; EMT, epithelial mesenchymal transition; VDR, vitamin D₃ receptor; fMLP, N-formylated peptides like fMLP.

As expected, many substrate metabolism pathways showed more clear-cut alterations based on metabolomic analysis. In contrast, the pathway analysis based on transcriptome showed more robust changes than those noted for many other pathways, such as prostaglandin, PPAR, immune response, and muscle contraction.

To obtain further information on the effect of such altered pathways on the biological processes during insulin deficiency, metabolomics data were overlaid with the transcriptomics data to depict a metabolic network, as illustrated in Fig. 4. The network model was built using canonical pathways (Fig. 3A and B). The association of genes and metabolites involved in PPAR transcription pathway was found to be one of the significant pathways affected at both the metabolic and the transcript levels during insulin deficiency (Figs. 3A and 4A). PPAR network showed differential expression of transcripts of cAMP-dependent protein kinase (PKA), protein kinase B (Akt), prostaglandin 12 synthase, X-linked inhibitor of apoptosis, mitogen-activated protein kinase kinase kinase 7 (TAK1), and metabolites such as long chain fatty acids, prostaglandin-2, leukotriene, and hydroperoxylinoleic acid (Fig. 4A). The associations of prostaglandins, HEPTE, fatty acid

metabolites, and arachidonic acid biosynthesis are all interconnected, thus affecting other metabolic responses, such as carbohydrate, lipid homeostasis, insulin receptor signaling, and transforming growth factor-β signaling. A molecular network was also generated for the insulin signaling pathways, which also showed coclustering of gene transcripts, e.g., *PKA*, *PDE3B*, *Akt*, and *ACSL1* and metabolites, such as glucose, glucose-6-phosphate, citric acid, and others (Fig. 4B).

DISCUSSION

A nontargeted mass spectrometry-based metabolic profiling in T1D showed that insulin deficiency altered several known and unknown metabolites and various putative metabolic pathways. Many but not all of these alterations were normalized by insulin treatment. Moreover, additional metabolites and pathways were found to be affected by insulin treatment. The confirmation of previously reported metabolic pathways affected by insulin based on multiple analytical approaches supports the validity of the metabolomic analysis of plasma samples. The revelation of previously unknown pathways affected by insulin is likely

B



FIG. 3. Continued

to stimulate novel hypotheses-based research. The integrated analysis of the altered metabolic pathways based on plasma metabolomics and skeletal muscle microarray-based gene transcriptomics showed significant concordance.

Insulin withdrawal in T1D caused elevation of levels of many known metabolites such as ketogenic and gluconeogenic amino acid, BCAA, glycerol, and β -hydroxybutyrate suggesting an increased rate of proteolysis, lipolysis, and ketogenesis. These results are consistent with previous reports based on both nuclear magnetic resonance spectroscopy and LC coupled with tandem mass spectroscopy in T1D and the insulin resistance state (23,32). The current approach also showed that major molecular and cellular functions affected by insulin deficiency, as expected, were carbohydrate ($P < 0.00001$), lipid ($P < 0.0004$), molecular transport and amino acid ($P < 0.0004$), and nucleic acid metabolism ($P < 0.04$). In addition, many other known pathways such as tricarboxylic acid cycle and mitochondrial ketone bodies biosynthesis and degradation were found to be affected. In general, many altered pathways that switch from anabolic to catabolic mode, whereas insulin secretion after a glucose meal exhibited a reverse effect (32).

The current study showed various metabolites and pathways that were previously not recognized as affected by insulin action. Among such affected pathways is prostaglandin metabolism with its wide range of impacts on various functions including platelet aggregation that may lead to vascular complications. A previous study reported high levels of plasma prostaglandin- E_2 and prostaglandin- F_2 and low levels of serum dihomo- γ -linolenic acid and arachidonic acid in association with increased platelet aggregation in diabetic children (33). The oxidative

metabolism of arachidonic acid was found to promote insulin release from pancreatic β -cells (34,35), and prostaglandin was postulated to play a potential role in the pathophysiology of type 2 diabetes (36,37). A recent report showed that insulin deficiency affected the arachidonic metabolism pathway (38,39). Arachidonic acid is converted to prostaglandins, leukotrienes, and lipoxins, of which prostaglandin-E and leukotrienes are potent proinflammatory lipid mediators and are also linked to hepatic steatosis (40,41). Altered regulation of the oxidized lipids such as eicosatetraenoic acid and its hydroxylated form HETE was observed in insulin deficiency in the current study. 5-eicosatetraenoic acid is an intermediate product of leukotriene-A4 and might alter immune response and leukotriene b4 biosynthesis. They are also involved in mediating inflammation and induced the adhesion and activation of leukocytes on the endothelium, allowing them to bind to and cross into tissue (41). The complications of diabetes involving inflammation and endothelial dysfunction may be mediated by alterations in the prostaglandin pathways (37,42).

The lipoxin pathway was also found to be affected by insulin deficiency and inhibitory action of lipoxins and superoxide production in the neutrophil, which might be manifested by a diminished inflammatory response in T1D (43). The current study also noted a substantial upregulation of aldosterone biosynthesis and metabolic pathways. This is of considerable interest, as aldosterone excess has been extensively studied, shown to be a major cause of cardiovascular complications in many insulin resistance conditions, and may contribute to vascular complications in T1D.

The current metabolomics approach measures not only metabolites derived from endogenous cellular metabolism

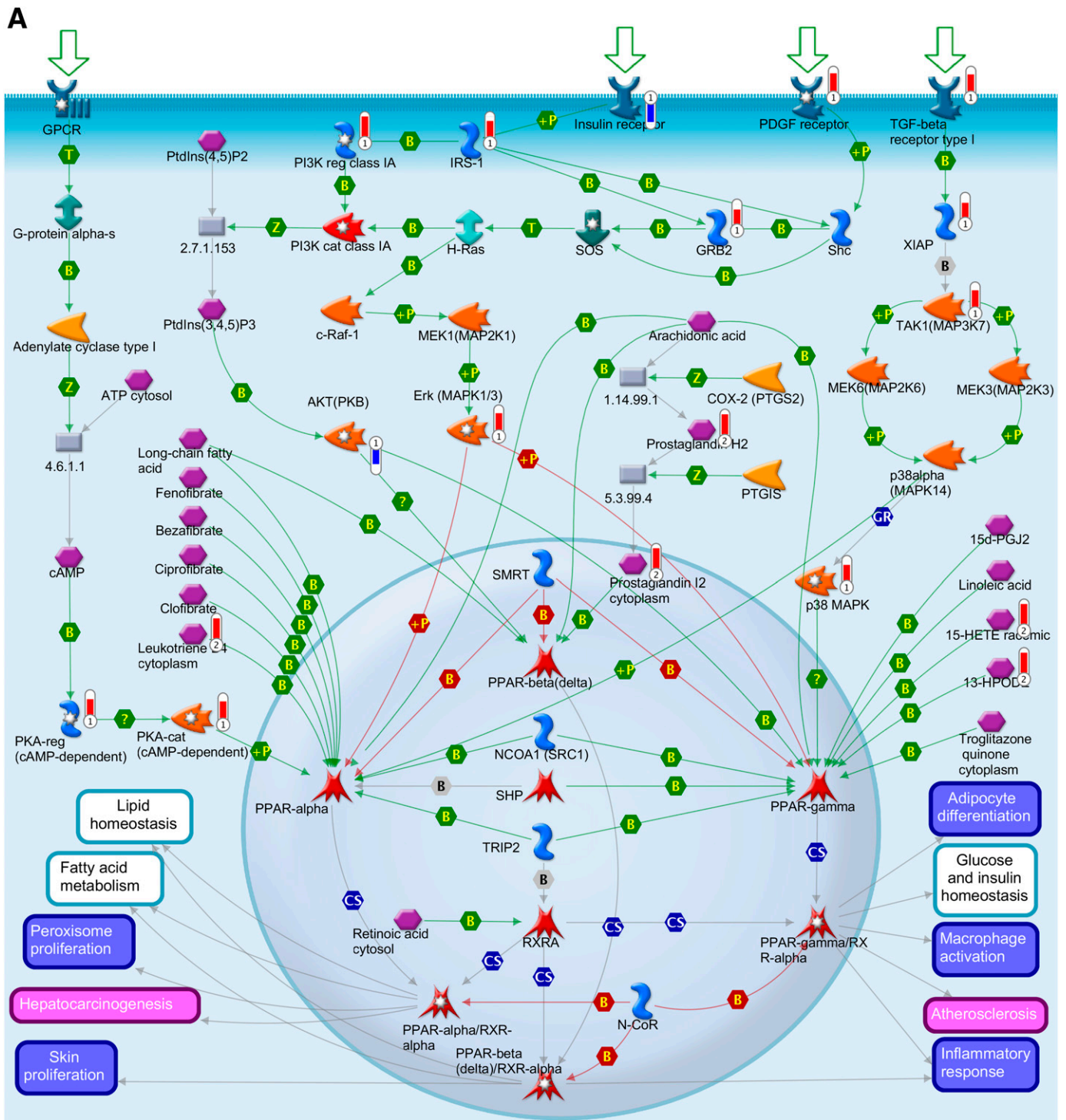


FIG. 4. Integration of the metabolomics with transcriptomics data and their superimposition to build metabolic networks. **A:** Metabolic network of PPAR transcription pathway, which is connected to other metabolic processes such as lipid homeostasis, glucose, fatty acid metabolism, and inflammatory response. **B:** Network model of downstream of insulin-signaling pathways. The metabolites and the gene names shown in red are upregulated, and the same shown in blue are downregulated during insulin deficiency. B, binding; C, cleavage; CoA, coenzyme A; Erk, extracellular signal-related kinase; HPODE, hydroperoxylinoleic acid; IE, influence on expression; MAP, mitogen-activated protein; MAPK, MAP kinase; PDGF, platelet-derived growth factor; PI3K, phosphatidylinositol 3-kinase; PKA, cAMP-dependent protein kinase; PKB, protein kinase B; P-, dephosphorylation; RXR, retinoid X receptor; SREBP1c, sterol regulatory element-binding protein 1c; T, transformation; TGF, transforming growth factor; TR, transcription regulation; +P, phosphorylation; Z, catalysis; GPCR, G protein-coupled receptor; 15d-PGJ2, deoxy-delta prostaglandin J2; PDK/PDK1, 3-phosphoinositide-dependent protein kinase -1; ACACA, acetyl-CoA carboxylase; ACSL, acyl-CoA synthetase long-chain family members; ACLY, ATP citrate lyase; BCAA, branch chain amino acid; CISY, citrate synthase; DAG, diacylglycerol; ELOVL, elongation-of-very-long-chain-fatty acids; EMT, epithelial-mesenchymal transition; BEH, ethylene-bridged hybrid; 4E-BP1, eukaryotic translation initiation factor 4E binding protein 1; FADS1, fatty acid desaturase 1; FASN, fatty acid synthase; GSK3 β , glycogen synthase kinase 3; GNAS, G protein α -dependent adenylate cyclase; GRB2, growth factor receptor-bound protein 2; H-Ras, Harvey rat sarcoma viral oncogene homolog; HGF, hepatocyte growth factor; HXK, hexokinase; HSS, high-strength silica; HODE, hydroxyoctadecadienoic acid; INSIG2, insulin-induced gene 2; IRS-1 and IRS-2, insulin receptor substrates-1 and -2; TRIP, mediator complex subunit 1; MEK/MAP1, mitogen-activated protein kinase 1; NCOA1, nuclear receptor coactivator 1; NR1/SRC1, nuclear receptor coactivator 1; N-CoR, nuclear receptor corepressor; SMRT, nuclear receptor corepressors; NUDT1, nudix (nucleoside diphosphate-linked moiety X)-type motif 1; PtdIns(3,4,5)P₃, phosphatidylinositol 3,4,5-triphosphate; PI3K, phosphatidylinositol 3-kinase;

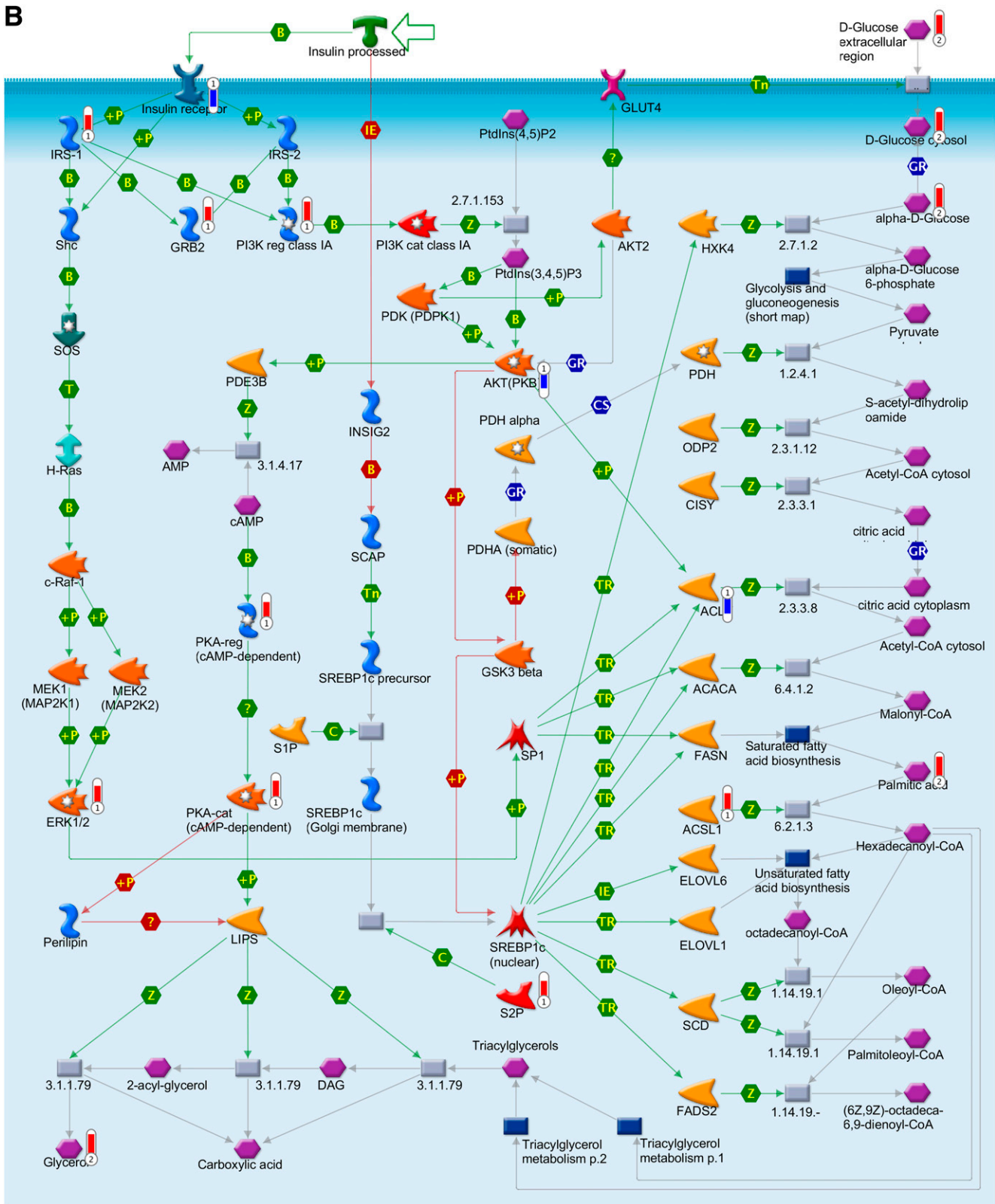


FIG. 4. (Continued) PtdIns(4,5)P₂, phosphatidylinositol 4,5-biphosphate; PGE, prostaglandin; PTGIS, prostaglandin I₂ (prostacyclin) synthase; PDGHS, prostaglandin-endoperoxide synthase 2 prostaglandin G/H synthase; COX2, cyclooxygenase 2; PDHA, pyruvate dehydrogenase (lipoamide) α1; QCs, quality controls; RARs, retinoic acid receptors; RXRA, retinoid X nuclear receptor (α); SHC, Src homology 2 domain containing transforming protein 1; SHP, small heterodimer partner; SOS, son of sevenless protein homologs 1 and 2; c-Raf-1, gene homolog 1; XIAP, X-linked inhibitor of apoptosis.

TABLE 3
Putative pathways that are altered after insulin treatment in T1D with respect to ND individuals

Maps	Metabolites	<i>P</i>	Ratio
HETE and HPETE biosynthesis and metabolism	Arachidonic acid, HETE, HPETE	6.892e ⁻⁸	10:80
Prostaglandin biosynthesis and metabolism and immune response	Prostaglandin, arachidonic acid, HETE, HPETE	1.075e ⁻⁵	9:101
Leucine, isoleucine, and valine (BCAA) metabolism	Leucine, isoleucine, valine, oxovaline	4.079e ⁻⁶	9:54
Histidine-glutamate-glutamine metabolism (L)-Alanine, (L)-cysteine, and (L)-methionine metabolism	Histidine, alanine, oxoglutaric acid, Alanine, cystine, oxoglutarate, glutamate	5.510e ⁻⁵	9:96
GABA biosynthesis and metabolism	Aminobutyrate, glutamate, glutamine, oxoglutarate	4.215e ⁻⁴	6:56
Transcription of PPAR pathway	Prostaglandin, leukotriene 4, HETE, HPODE	9.827e ⁻⁴	6:55
Muscle contraction: nNOS signaling in skeletal muscle	Acetylcholine, glucose, arginine, acetate, citrate, phosphoinositol	4.306e ⁻³	5:61
Leukotriene 4 biosynthesis and metabolism	Prostaglandin, arachidonic acid, HETE, HPETE	2.618e ⁻²	5:43
Regulation of lipid metabolism: insulin regulation of fatty acid metabolism	Hydroxybutyrate, acetoacetate, glycerol, glycerol phosphate, palmitic acid	9.993e ⁻⁴	5:44
Niacin-HDL metabolism	Nicotinamide, niacin, glycerol	3.885e ⁻⁴	6:55
Tricarboxylic acid	Citrate, ketoglutarate, pyruvate, acetoacetate	4.094e ⁻³	6:47
		5.496e ⁻³	5:51

P value is the mean of *P* values of three pairs of study groups depicting significance of the pathway, and ratio is the number of compounds identified to the total number of metabolites present in a pathway. HPODE, hydroperoxylinoleic acid; nNOS, neuronal nitric oxide synthase.

but also those derived exogenously from drugs, foods, and cosmetics, etc. A list of medications taken by the participants and those detected in plasma is given (Supplementary Table 1). Surprisingly, we noted that among the metabolites that showed significant differences between I⁺ and I⁻ were morphine and coniine. Since the identification of these compounds is putative based on mass (*m/z*), it is possible that molecules may be reported with *m/z* identical to that of morphine and coniine. It is known that endogenous opioids such as endorphins are measured in plasma in individuals after glycogen-depleting aerobic exercise (44,45). It remains unclear whether insulin deprivation in T1D and associated glycogen depletion may increase endorphin secretion. Endorphin also has substantial structural similarity in terms of amino acid sequence to that of adrenocorticotrophic hormone, and many other alkaloids might have a structure similar to that of coniine. However, the importance of these findings warrants more detailed studies.

Insulin treatment corrected the levels of most of the altered metabolites, but some of the metabolites and metabolic pathways (Fig. 2B and Table 3) remained unaffected. In addition, insulin treatment showed changes in seven metabolic pathways that were not previously observed to be affected in T1D during insulin treatment (Fig. 2B). The additional group of metabolites altered by insulin treatment (ND vs. I⁺) included many organic acids, glucogenic amino acids, bile acids, purine, pyrimidine, phosphatidylcholine, ethanolamine, carnitine, and creatinine (Supplementary Table 7). Several of these metabolites are involved in hepatic metabolism and lipid metabolic processes in adipose tissue (46,47). The potential impact of these altered pathways in T1D after insulin treatment requires future investigation. Systemic versus prehepatic insulin administration altered energy and protein metabolism in diabetic dogs (48). We have shown the effects of short-term tight glycemic control by insulin, but it remains to be determined whether long-term insulin treatment will show persistent changes in these pathways. Higher glucagon levels in I⁻ compared with I⁺ may have contributed

to some of the changes (49,50), although insulin deficiency is likely the predominant factor.

Previous studies reported that cessation of insulin treatment is associated with higher oxidative metabolism (16) but reduced skeletal muscle ATP production (24), thus creating an environment of high oxidative stress. This higher oxidative metabolism and catabolism of many amino acids (50) were also shown to be at least partially related to hyperglucagonemia (49). Glucagon has no receptors in skeletal muscle; therefore, it is likely that these effects of glucagon may have occurred in liver but not in skeletal muscle. Insulin deficiency in T1D individuals has also been shown to accelerate the catabolism of many amino acids, especially of BCAA in skeletal muscle (17). The changes in plasma metabolites observed therefore represent not only processes occurring in skeletal muscle but also processes in multiple other organs, especially in liver. We have examined whether findings from plasma metabolite-based pathway analysis are in agreement with those derived from skeletal muscle gene transcriptome.

The current study demonstrated concordance of 16 canonical pathways that are altered by insulin deficiency based on metabolomics versus transcriptomics (Fig. 3A). Moreover, similar alterations of the pathways between I⁺ T1D and ND were also observed (Fig. 3B). Metabolic response displayed a much higher level of specificity than the transcriptomics data, which may be due to the capacity of the metabolites to respond faster to short-term insulin deprivation than muscle transcription of genes. Metabolomics of human plasma is a reflection of the spillover from various organs from all over the body, whereas the transcriptomics of muscle tissue only depicts the localized changes in mRNA levels. Thus, synergy of metabolites and genes and the canonical correlation approaches enabled us to demonstrate the effect of coordinated changes of the transcriptome and the metabolic processes.

The integration of the data from both analyses allowed us to build metabolic networks of PPAR and insulin-signaling pathway as shown in Fig. 4. Of interest, pathway

analysis based on both plasma metabolites and gene transcriptome demonstrated highly significant ($P < 0.004$) differences of PPAR pathway between I⁻ and I⁺ T1D/ND participants. The different isoforms of PPAR were not distinguished by the pathway-enrichment analysis. The metabolites involved in the specific PPAR- α , - β , and - γ pathways require further investigation.

The current study confirmed the validity of the non-targeted plasma metabolomic profiling by demonstrating that this single plasma analysis could identify most pathways previously reported based on multiple approaches over many years of research. In addition, the significant concordance of pathways based on plasma metabolites and skeletal muscle transcriptome supports the notion that plasma metabolites are chemical fingerprints of cellular metabolites and pathways. The novel pathway affected by insulin and the demonstration of alteration of many metabolites and pathways affected by insulin treatment indicate potential therapeutic targets for the high morbidity and mortality in T1D individuals despite improved glycemic control.

ACKNOWLEDGMENTS

This research was supported by National Institutes of Health Grant R01 DK41973 and by Center for Translational Science Activities Grant UL1 RR024150-01.

No potential conflicts of interest relevant to this article were reported.

T.D. designed the experiment, undertook sample preparation, performed laboratory analyses using UPLC-ToF MS, analyzed data and pathway results, interpreted the findings, and wrote the manuscript. H.S.C. performed statistical analysis, analyzed data, interpreted the findings, and wrote the statistical section in the manuscript. L.E.W. contributed to the analysis of the data and contributed to the manuscript. A.G. analyzed data and samples and read the manuscript. X.-M.T.P. was involved in the analysis of the samples and contributed to the manuscript. G.C.F. was involved in the analysis, interpretation of data, and writing the manuscript. Y.C.K. was involved in the collection of samples and interpretation of data and contributed to the manuscript. Z.S. helped with pathway analysis and contributed to the manuscript. Y.W.A. performed microarray analysis and interpreted the results. J.-P.A.K. led the Bioinformatics team, who analyzed data, and contributed to the writing of the manuscript. K.S.N. conceived and designed the experiment, coordinated and supervised data collection and analysis, interpreted the findings, and wrote the manuscript. K.S.N. is the guarantor of this work and, as such, had full access to all the data in the study and takes responsibility for the integrity of the data and the accuracy of the data analysis.

REFERENCES

- Tessari P, Nosadini R, Trevisan R, et al. Defective suppression by insulin of leucine-carbon appearance and oxidation in type 1, insulin-dependent diabetes mellitus. Evidence for insulin resistance involving glucose and amino acid metabolism. *J Clin Invest* 1986;77:1797-1804
- Rizza RA, Jensen MD, Nair KS. Type I diabetes mellitus (insulin-dependent diabetes mellitus). In *Handbook of Physiology*. New York, Oxford University Press, 2001, p. 1093-1114
- Melloul D, Marshak S, Cerasi E. Regulation of insulin gene transcription. *Diabetologia* 2002;45:309-326
- Sreekumar R, Halvatsiotis P, Schimke JC, Nair KS. Gene expression profile in skeletal muscle of type 2 diabetes and the effect of insulin treatment. *Diabetes* 2002;51:1913-1920
- Kimball SR, Jefferson LS. Cellular mechanisms involved in the action of insulin on protein synthesis. *Diabetes Metab Rev* 1988;4:773-787
- Jaleel A, Henderson GC, Madden BJ, et al. Identification of de novo synthesized and relatively older proteins: accelerated oxidative damage to de novo synthesized apolipoprotein A-1 in type 1 diabetes. *Diabetes* 2010;59:2366-2374
- Kahn CR. Diabetes. Causes of insulin resistance. *Nature* 1995;373:384-385
- Bain JR, Stevens RD, Wenner BR, Ilkayeva O, Muoio DM, Newgard CB. Metabolomics applied to diabetes research: moving from information to knowledge. *Diabetes* 2009;58:2429-2443
- Wang X, Jia S, Geoffrey R, Alemzadeh R, Ghosh S, Hessner MJ. Identification of a molecular signature in human type 1 diabetes mellitus using serum and functional genomics. *J Immunol* 2008;180:1929-1937
- Gehlenborg N, O'Donoghue SI, Baliga NS, et al. Visualization of omics data for systems biology. *Nat Methods* 2010;7(Suppl.):S56-S68
- Connor SC, Hansen MK, Corner A, Smith RF, Ryan TE. Integration of metabolomics and transcriptomics data to aid biomarker discovery in type 2 diabetes. *Mol Biosyst* 2010;6:909-921
- Zhang X, Wang Y, Hao F, et al. Human serum metabolomic analysis reveals progression axes for glucose intolerance and insulin resistance statuses. *J Proteome Res* 2009;8:5188-5195
- Zhang S, Nagana Gowda GA, Asiago V, Shanaiah N, Barbas C, Raftery D. Correlative and quantitative ¹H-NMR-based metabolomics reveals specific metabolic pathway disturbances in diabetic rats. *Anal Biochem* 2008;383:76-84
- Wang TJ, Larson MG, Vasani RS, et al. Metabolite profiles and the risk of developing diabetes. *Nat Med* 2011;17:448-453
- Zhao X, Fritsche J, Wang J, et al. Metabonomic fingerprints of fasting plasma and spot urine reveal human pre-diabetic metabolic traits. *Metabolomics* 2010;6:362-374
- Nair KS, Halliday D, Garrow JS. Increased energy expenditure in poorly controlled type 1 (insulin-dependent) diabetic patients. *Diabetologia* 1984;27:13-16
- Nair KS, Ford GC, Ekberg K, Fernqvist-Forbes E, Wahren J. Protein dynamics in whole body and in splanchnic and leg tissues in type I diabetic patients. *J Clin Invest* 1995;95:2926-2937
- Felig P, Wahren J, Sherwin R, Hendler R. Insulin, glucagon, and somatostatin in normal physiology and diabetes mellitus. *Diabetes* 1976;25:1091-1099
- Polonsky KS, Rubenstein AH. C-peptide as a measure of the secretion and hepatic extraction of insulin. Pitfalls and limitations. *Diabetes* 1984;33:486-494
- Kubota T, Kubota N, Kumagai H, et al. Impaired insulin signaling in endothelial cells reduces insulin-induced glucose uptake by skeletal muscle. *Cell Metab* 2011;13:294-307
- DeFronzo RA, Tobin JD, Andres R. Glucose clamp technique: a method for quantifying insulin secretion and resistance. *Am J Physiol* 1979;237:E214-E223
- Jaleel A, Klaus KA, Morse DM, et al. Differential effects of insulin deprivation and systemic insulin treatment on plasma protein synthesis in type 1 diabetic people. *Am J Physiol Endocrinol Metab* 2009;297:E889-E897
- Lanza IR, Zhang S, Ward LE, Karakelides H, Raftery D, Nair KS. Quantitative metabolomics by H-NMR and LC-MS/MS confirms altered metabolic pathways in diabetes. *PLoS ONE* 2010;5:e10538
- Karakelides H, Asmann YW, Bigelow ML, et al. Effect of insulin deprivation on muscle mitochondrial ATP production and gene transcript levels in type 1 diabetic subjects. *Diabetes* 2007;56:2683-2689
- Nair KS, Halliday D, Griggs RC. Leucine incorporation into mixed skeletal muscle protein in humans. *Am J Physiol* 1988;254:E208-E213
- Chen J, Zhao X, Fritsche J, et al. Practical approach for the identification and isomer elucidation of biomarkers detected in a metabolomic study for the discovery of individuals at risk for diabetes by integrating the chromatographic and mass spectrometric information. *Anal Chem* 2008;80:1280-1289
- Sana TR, Fischer S, Wohlgenuth G, et al. Metabolomic and transcriptomic analysis of the rice response to the bacterial blight pathogen *Xanthomonas oryzae* pv. *oryzae*. *Metabolomics* 2010;6:451-465
- Asmann YW, Stump CS, Short KR, et al. Skeletal muscle mitochondrial functions, mitochondrial DNA copy numbers, and gene transcript profiles in type 2 diabetic and nondiabetic subjects at equal levels of low or high insulin and euglycemia. *Diabetes* 2006;55:3309-3319
- Balagopal P, Schimke JC, Ades P, Adey D, Nair KS. Age effect on transcript levels and synthesis rate of muscle MHC and response to resistance exercise. *Am J Physiol Endocrinol Metab* 2001;280:E203-E208
- Rubin DB (Ed.). *Multiple Imputation for Nonresponse in Surveys*. New York, John Wiley & Sons, 1987, p. 75-107
- Schuerer S, Tranchevent LC, Dengler U, Moreau Y. Large-scale benchmark of Endeavour using MetaCore maps. *Bioinformatics* 2010;26:1922-1923
- Shaham O, Wei R, Wang TJ, et al. Metabolic profiling of the human response to a glucose challenge reveals distinct axes of insulin sensitivity. *Mol Syst Biol* 2008;4:214

33. Arisaka M, Arisaka O, Fukuda Y, Yamashiro Y. Prostaglandin metabolism in children with diabetes mellitus. I. Plasma prostaglandin E₂, F₂ alpha, TXB₂, and serum fatty acid levels. *J Pediatr Gastroenterol Nutr* 1986;5: 878–882
34. Robertson RP. Arachidonic acid metabolite regulation of insulin secretion. *Diabetes Metab Rev* 1986;2:261–296
35. Persaud SJ, Muller D, Belin VD, et al. The role of arachidonic acid and its metabolites in insulin secretion from human islets of langerhans. *Diabetes* 2007;56:197–203
36. Robertson RP, Chen M. A role for prostaglandin E in defective insulin secretion and carbohydrate intolerance in diabetes mellitus. *J Clin Invest* 1977;60:747–753
37. Robertson RP. Prostaglandins, glucose homeostasis, and diabetes mellitus. *Annu Rev Med* 1983;34:1–12
38. Xie Z, Li H, Wang K, et al. Analysis of transcriptome and metabolome profiles alterations in fatty liver induced by high-fat diet in rat. *Metabolism* 2010;59:554–560
39. Ma K, Nunemaker CS, Wu R, Chakrabarti SK, Taylor-Fishwick DA, Nadler JL. 12-lipoxygenase products reduce insulin secretion and beta-cell viability in human islets. *J Clin Endocrinol Metab* 2010;95:887–893
40. Li JH, Chou CL, Li B, et al. A selective EP₄ PGE₂ receptor agonist alleviates disease in a new mouse model of X-linked nephrogenic diabetes insipidus. *J Clin Invest* 2009;119:3115–3126
41. Takahashi HK, Zhang J, Mori S, et al. Prostaglandin E₂ inhibits advanced glycation end product-induced adhesion molecule expression on monocytes, cytokine production, and lymphocyte proliferation during human mixed lymphocyte reaction. *J Pharmacol Exp Ther* 2010;334:964–972
42. Metz S, VanRollins M, Strife R, Fujimoto W, Robertson RP. Lipoxygenase pathway in islet endocrine cells. Oxidative metabolism of arachidonic acid promotes insulin release. *J Clin Invest* 1983;71:1191–1205
43. Filep JG, Zouki C, Petasis NA, Hachicha M, Serhan CN. Anti-inflammatory actions of lipoxin A(4) stable analogs are demonstrable in human whole blood: modulation of leukocyte adhesion molecules and inhibition of neutrophil-endothelial interactions. *Blood* 1999;94:4132–4142
44. Gambert SR, Garthwaite TL, Pontzer CH, et al. Running elevates plasma beta-endorphin immunoreactivity and ACTH in untrained human subjects. *Proc Soc Exp Biol Med* 1981;168:1–4
45. Carr DB, Bullen BA, Skrinar GS, et al. Physical conditioning facilitates the exercise-induced secretion of beta-endorphin and beta-lipotropin in women. *N Engl J Med* 1981;305:560–563
46. Li LO, Hu YF, Wang L, Mitchell M, Berger A, Coleman RA. Early hepatic insulin resistance in mice: a metabolomics analysis. *Mol Endocrinol* 2010; 24:657–666
47. Le Bouter S, Rodriguez M, Guigal-Stephan N, et al. Coordinate transcriptomic and metabolomic effects of the insulin sensitizer rosiglitazone on fundamental metabolic pathways in liver, soleus muscle, and adipose tissue in diabetic db/db mice. *PPAR Res* 10 October 2010 [Epub ahead of print]
48. Freyse EJ, Fischer U, Knospe S, Ford GC, Nair KS. Differences in protein and energy metabolism following portal versus systemic administration of insulin in diabetic dogs. *Diabetologia* 2006;49:543–551
49. Charlton MR, Adey DB, Nair KS. Evidence for a catabolic role of glucagon during an amino acid load. *J Clin Invest* 1996;98:90–99
50. Charlton M, Nair KS. Protein metabolism in insulin-dependent diabetes mellitus. *J Nutr* 1998;128(Suppl.):323S–327S